Chemical characterization of ambient aerosol collected during the northeast monsoon season over the Arabian Sea: Anions and cations

Anne M. Johansen
Department of Chemistry, Central Washington University, Ellensburg, Washington, USA

Michael R. Hoffmann
Environmental Science and Engineering, California Institute of Technology, Pasadena, California, USA

Received 26 August 2003; revised 8 December 2003; accepted 31 December 2003; published 4 March 2004.

[1] Ambient aerosol samples were collected over the Arabian Sea during the month of March 1997, aboard the German R/V *Sonne*, as part of the German JGOFS project (Joint Global Ocean Flux Study). This is the third study in a series of analogous measurements taken over the Arabian Sea during different seasons of the monsoon. Dichotomous high volume collector samples were analyzed for anions and cations upon return to the laboratory. Anthropogenic pollutant concentrations were larger during the first part of the cruise, when air masses originated over the Indian subcontinent. Total NSS-SO_4^{2-} concentrations amounted to 2.94 ± 1.06 μg m^{-3} of which 92.1 ± 4.5% was present in the fine fraction. NSS-SO_4^{2-} source apportionment analysis with multivariate linear regression models revealed that in the coarse fraction half is biogenically and half anthropogenically derived, while in the fine fraction only 6% seemed of biogenic origin and 84% anthropogenic and 10% crustal in nature. Chloride deficits up to 99.1% in the fine fraction were observed. The average Cl^- deficit in the fine fraction was 89.0 ± 9.4%, potentially related to NSS-SO_4^{2-} acid displacement and Cl reactive species formation, while in the coarse fraction it was 25.6 ± 21.3%, with NO_3^- being the preferred species for acid displacement. *INDEX TERMS:* 0305 Atmospheric Composition and Structure: Aerosols and particles (0345, 4801); 0335 Atmospheric Composition and Structure: Ion chemistry of the atmosphere (2419, 2427); 0365 Atmospheric Composition and Structure: Troposphere—composition and chemistry; 4801 Oceanography: Biological and Chemical: Aerosols (0305); *KEYWORDS:* marine aerosol, ions, Arabian Sea

Citation: Johansen, A. M., and M. R. Hoffmann (2004), Chemical characterization of ambient aerosol collected during the northeast monsoon season over the Arabian Sea: Anions and cations, *J. Geophys. Res.*, *109*, D05305, doi:10.1029/2003JD004111.

1. Introduction

[2] The present study is part of a larger set of field observations collected over the Arabian Sea to determine the chemical composition of atmospheric aerosol particles during different seasons of the monsoon [*Johansen and Hoffmann*, 2003; *Johansen et al.*, 1999; *Siefert et al.*, 1999].

[3] The northern Indian Ocean is subject to a strong biannual reversal pattern in the low-level winds associated with the Indian monsoon [*Ackerman and Cox*, 1989; *Findlater*, 1969, 1971; *Middleton*, 1986a, 1986b]. The monsoon flow pattern, which is largely driven by the heat gradient between the Indian subcontinent and the ocean, is typified by SW winds during the northern hemisphere summer and NE winds during the northern hemisphere winter. The intermonsoon is classified as the period between the NE- and the SW-monsoons when no predominant wind pattern exists. Two previous studies of the SW- and intermonsoons showed that the direction of the airflow over the Arabian Sea affects both the abundance and composition of the aerosols [*Johansen et al.*, 1999; *Siefert et al.*, 1999]. These studies found that during the SW-monsoon the air is mainly marine derived originating from the southwestern Indian Ocean, while during the intermonsoon the air masses contain a considerable amount of crustal and anthropogenic material originating mainly from the Arabian Peninsula and other parts of the Middle East. Aerosol trace metal composition from the current cruise was presented in Johansen and Hoffmann [*Johansen and Hoffmann*, 2003], and revealed that during the NE-monsoon an appreciable amount of anthropogenic material is advected over the Arabian Sea. In the present study anion and cation concentrations in both coarse and fine fractions were analyzed and interpreted in the context of the trace metal data.

[4] The recent extensive study of the chemical and physical properties of the atmosphere over the Arabian Sea during the NE-monsoons of 1998 and 1999, Indian Ocean Experiment (INDOEX), provides vast information in this geographic region. A large number of studies on the

0148-0227/04/2003JD004111

chemical composition of aerosols during INDOEX have been published recently [*Ball et al.*, 2003; *Chand et al.*, 2003; *Clarke et al.*, 2002; *Eldering et al.*, 2002; *Gabriel et al.*, 2002; *Nair et al.*, 2001; *Norman et al.*, 2003; *Rao et al.*, 2001; *Reddy and Venkataraman*, 2002a, 2002b; *Venkataraman et al.*, 2002, 2001]. Up until then, there were very few measurements of trace chemical species from the Indian Ocean. *Tindale and Pease* [1999] provide an overview of dust transport pathways and concentrations over the Arabian Sea, revealing that the input of dust to the region is highly dependent on season and location. *Savoie et al.* [1987] sampled nitrate, non-sea-salt-sulfate (NSS-SO_4^{2-}) and mineral aerosol during the NE- and spring intermonsoon of 1979 and found a strong gradient in the concentrations of the measured species, decreasing toward the south. They also detected large concentrations of NSS-Ca in the form of gypsum and suggested that the most likely sources are gypsiferous soils which are known to exist in some regions of the Thar, the Indian and the Arabian deserts. Photographs taken suggest that dust can be transported simultaneously from all these areas over the Arabian Sea. Large concentrations of NSS-Ca were also observed by *Naik et al.* [1991], *Johansen et al.* [1999], and *Savoie et al.* [1987], who determined it to be of crustal origin. *Johansen et al.* [1999] and *Savoie et al.* [1987] attributed it to gypsum.

[5] In the present study, we are interested in the chemical interactions between marine and continental aerosols. Of specific interest is to determine the relative contributions of anthropogenic and biogenic sources to NSS-SO_4^{2-}, and to monitor the acid displacement reaction that leads to volatilization of sea salt derived Cl in the presence of NO_3^- and NSS-SO_4^{2-}. The interest in NSS-SO_4^{2-} particles in the submicrometer size range stems from their influence on the radiation balance of the atmosphere [*Charlson et al.*, 1987] in the form of cloud condensation nuclei (CCN). Since NSS-SO_4^{2-} may be of anthropogenic or biogenic origin, latter produced from the $OH^\bullet$ and $NO_3^\bullet$ radical oxidation of dimethyl sulfide (DMS) [*Berresheim et al.*, 1995; *Hynes et al.*, 1986; *Turnipseed and Ravishankara*, 1993; *Yin et al.*, 1990], it is essential that the relative contributions of these two sources be quantified. However, not all of this NSS-SO_4^{2-} may be directly affecting the albedo as sea-salt particles may act as seeds for the uptake and oxidation of sulfur gases and deposition of condensable sulfate vapors [*Keene et al.*, 1998; *McInnes et al.*, 1994], and thus contributing to the removal of gaseous sulfur species that may have otherwise have formed CCN [*Vogt et al.*, 1996]. This would result in a reduction of feedback between greenhouse warming, oceanic DMS emissions and increased could albedo.

[6] The interest in characterizing the sea-salt component is partly due to its ability to strongly influence the oxidative properties of aerosol particles in the marine boundary layer through the production of halogen radicals [*Fan and Jacob*, 1992; *Finlayson-Pitts et al.*, 1989; *Graedel and Keene*, 1995; *Keene et al.*, 1996; *Pszenny et al.*, 1993; *Sander and Crutzen*, 1996; *Vogt et al.*, 1996]. Reactive Cl can initiate photochemical reactions in an analogous manner to $OH^\bullet$ and have major consequences for the oxidation of hydrocarbons and DMS [*Keene et al.*, 1996, 1990; *Langer et al.*, 1996; *Pszenny et al.*, 1993; *Sander and Crutzen*, 1996; *Stickel et al.*, 1992; *Vogt et al.*, 1996], and in turn have an effect on greenhouse warming by modifying the atmospheric sulfur chemistry. Finally, the determination of anions is of direct importance in the discussion of atmospheric iron redox chemistry, which was presented in *Johansen and Hoffmann* [2003].

2. Experiment

2.1. Sampling Location and Period

[7] Atmospheric aerosol samples were collected over the Arabian Sea during the month of March of 1997. Sampling took place on board the German Research Vessel "Sonne", which sailed as part of the German Joint Global Ocean Flux Study (JGOFS) project. The cruise track, from Cochin/India to Muscat/Oman, is delineated in the plots in Figure 1. Back trajectory calculations were obtained from the German Weather Service in Hamburg, Germany, based on their isentropic Global-Modell (GME) with a resolution of 190 km [*Kottmeier and Fay*, 1998]. In order to get a sense of the vertical motion of the atmosphere each plot traces five different trajectories which correspond to different initial pressures (i.e., elevations) at the initial position. The highest trajectory, at 850 hPa, represents an altitude of about 1.5 km. The first part of the cruise was predominated by northeasterly winds, as expected, however, later in the cruise wind patterns changed such that the typical air mass originated over the Saudi Arabian peninsula and the Middle East, much like conditions encountered during the intermonsoon of 1995 [*Johansen et al.*, 1999; *Siefert et al.*, 1999]. This shift in atmospheric conditions is consistent with what scientists observed during the Indian Ocean Experiment (INDOEX) of 1999 and before [*Ball et al.*, 2003; *Clarke et al.*, 2002; *Rao et al.*, 2001; *Tindale and Pease*, 1999].

2.2. Aerosol Collection

[8] Ambient aerosol samples were collected with two different collectors. A high volume dichotomous virtual impactor (HVDVI) was used for the collection of trace metals in two discrete size fractions ($D_{p,50}$ = 3.0 μm) [*Johansen et al.*, 1999, 2000; *Siefert et al.*, 1999], whereby particles of diameter <3 μm will presently be defined as the fine particles and particles >3 μm in diameter will be denoted as the coarse particles. The HVDVI collector was constructed with polycarbonate using nylon screws in order to minimize trace metal contamination. The total flow rate was determined to 335 ± 15 l min^{-1}. The fine and coarse sample fractions were collected on two 90 millimeter diameter Teflon filters (Gelman Zefluor, 1 μm pore size). Total elemental composition, Fe(II) concentrations, and anion and cation abundances were determined for both fine and coarse filter samples.

[9] Two low volume collectors, which were operated at flow rates of 27 l min^{-1}, were used for collection of total aerosol mass. Inverted high density polyethylene bottles (2 L) served as rain shields for the Nucleopore polycarbonate 47 mm diameter filter holders which were loaded with acid-cleaned Gelman Zefluor filters (1 μm pore size).

[10] The aerosol collectors and lab equipment were acid-cleaned before use by following similar procedures

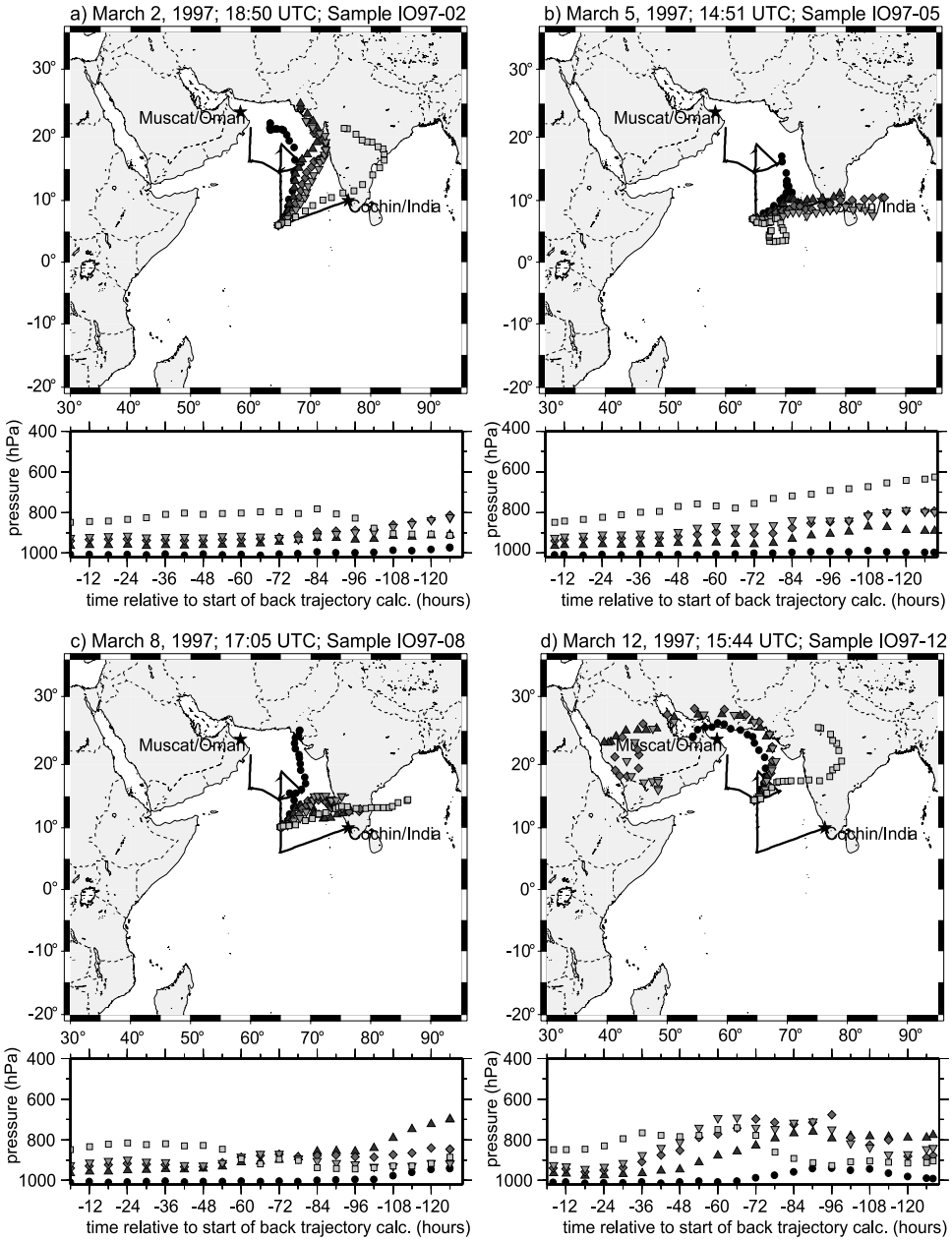

Figure 1. Five-day air mass back calculations at five different final elevations (based on pressure above sea level for (a) March 2, 1997; (b) March 5, 1997; (c) March 8, 1997; (d) March 12, 1997; (e) March 18, 1997; (f) March 20, 1997; (g) March 23, 1997; and (h) March 27, 1997.

as outlined by *Patterson and Settle* [1976] employing ultrapure acids from Seastar Chemicals (Sidney, B.C., Canada) and 18.2 MΩ-cm Milli-Q UV water. After Fe(II) analysis [*Johansen and Hoffmann*, 2003], the remainder of the filters were stored in acid-cleaned polystyrene petri dishes taped shut with Teflon tape, placed inside 2 plastic bags inside of a tupperware container and stored in a refrigerator during the cruise. After the cruise, the filters were sent back to Caltech (via air-freight, on dry ice) and stored in a freezer until analysis.

[11] A sector sampling system (by Campbell Scientific) controlled the operation of all collector pumps, thereby stopping collection of the aerosol collectors simultaneously when wind speed or wind direction were out of the defined sector. The data logger (CR10, Campbell Scientific) was programmed to shut the pumps off when the wind speed was $\leq$0.2 m s^{-1} and when the relative wind direction was more than ±60° off of the bow of the ship. In general, collected samples represent daily averages.

2.3. Chemical Analyses

2.3.1. Ion Analysis

[12] For the ion analyses, a small section of the high volume filter was first wetted with approximately 0.1 ml

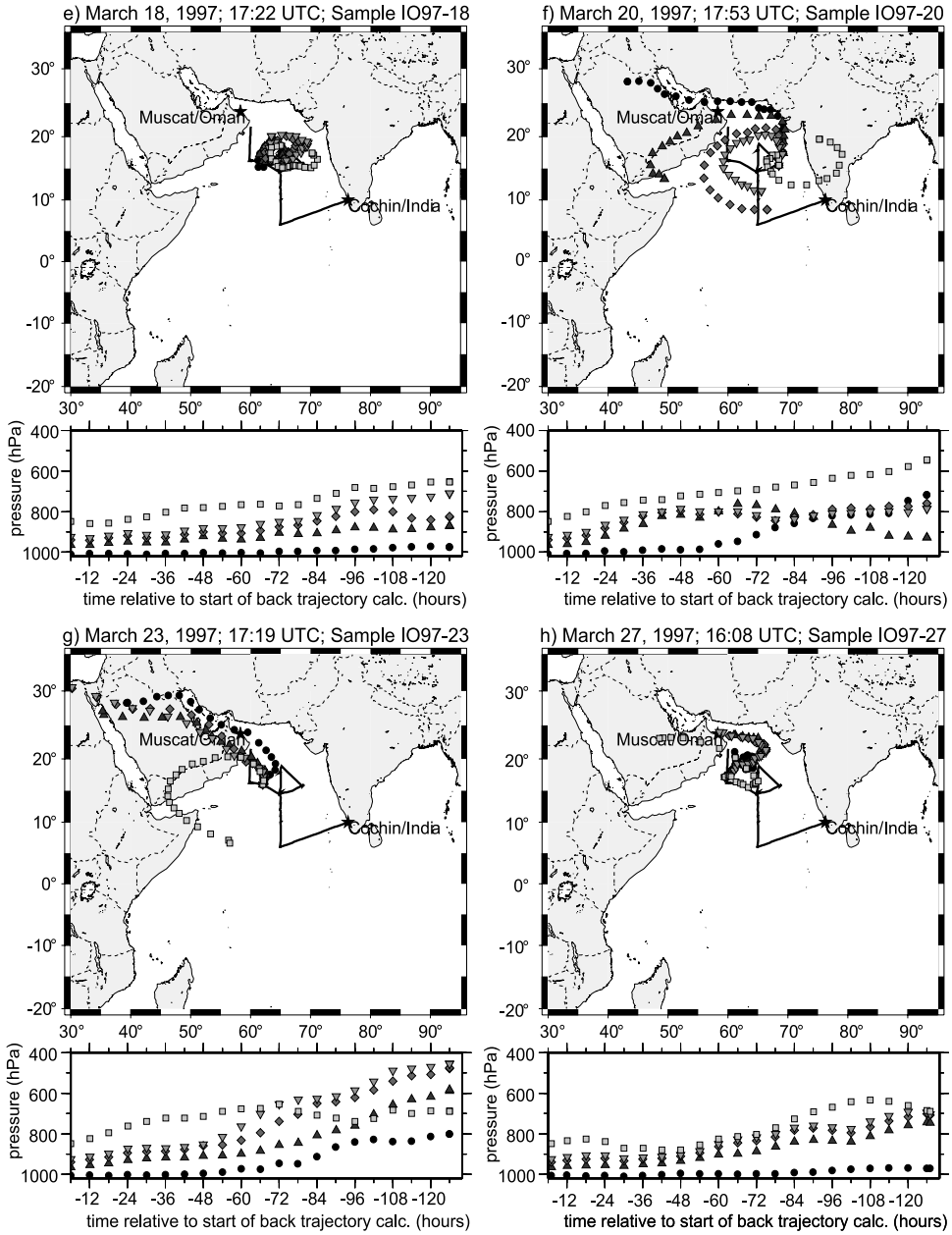

Figure 1. (continued)

ethanol then extracted overnight in 10 ml MQ water. Anions were separated and quantified with a Dionex Bio LC Ion Chromatograph (IC) using an IonPac AS11 separator column and the corresponding AG11 guard column. Organic and inorganic anions were eluted with a gradient pump and a combination of 4 eluents (5 mM NaOH, 100 mM NaOH, 100% MeOH, MQ H_2O) whereby the NaOH concentration was ramped from an initial 0.45 mM to a final 34.25 mM. The quantified anions included methanesulfonate (MSA), chloride, nitrate and sulfate. Fluoride, acetate, glycolate, formate, nitrite, bromide and oxalate were present at very low concentrations that were near the corresponding detection limits. Due to problems with the IC, 3 samples were not run correctly (fine IO97-08, fine IO97-18, and coarse IO97-19). The missing data is clearly indicated in the plots and the samples are removed from the data set when performing statistical analyses.

[13] Cations were separated and quantified isocratically with a DX 500 Ion Chromatograph (IC) with IonPac CS12/CG12 analytical and guard columns and a 20 mM MSA eluent. Sodium, ammonium, potassium, magnesium, and calcium concentrations were determined.

2.3.2. Elemental Analysis

[14] Elemental analysis of 32 elements (Na, Mg, Al, K, Ca, Sc, Ti, V, Cr, Mn, Fe, Ni, Cu, Zn, Ga, Ge, As, Se, Mo, Ru, Cd, Sn, Sb, Cs, Ba, La, Ce, Sm, Eu, Hf, Pb, and Th) was performed on the high volume filters with an HP 4500 ICP-MS (Inductively Coupled Mass Spectrometer). The filter digestion technique was presented by *Siefert et al.* [1999]. Only a few of the elements will be discussed in the

Table 1. Average, Minimum, and Maximum Atmospheric Anion and Cation Concentrations in Coarse, Fine, and Total Aerosol Fractions for Group 1 and 2 Samples[a]

	Group 1 (IO97-01-IO97-10)			Group 2 (IO97-11-IO97-27)		
Element	Average ± s.d.	Min.	Max.	Average ± s.d.	Min.	Max.
Cl^--coarse (μg m^{-3})	0.47 ± 0.22	0.15	0.90	0.75 ± 0.41	0.13	1.55
Cl^- fine (μg m^{-3})	0.02 ± 0.02	0.10	0.07	0.09 ± 0.08	0.03	0.40
NSS-Cl^--coarse (μg m^{-3})	−0.39 ± 0.16	−0.63	−0.15	−0.19 ± 0.10	−0.62	−0.02
NSS-Cl^--fine (μg m^{-3})	−0.60 ± 0.25	−1.14	−0.38	−0.50 ± 0.27	−0.64	−0.34
SO_4^{2-} -coarse (μg m^{-3})	0.35 ± 0.11	0.11	0.46	0.34 ± 0.12	0.18	0.58
SO_4^{2-}-fine (μg m^{-3})	3.70 ± 0.83	2.47	5.25	2.35 ± 1.24	1.46	3.16
NSS-SO_4^{2-}-coarse (μg m^{-3})	0.23 ± 0.08	0.06	0.33	0.18 ± 0.10	0.04	0.33
NSS-SO_4^{2-}-fine (μg m^{-3})	3.61 ± 0.81	2.41	5.09	2.27 ± 1.22	1.36	3.11
NO_3^--coarse (μg m^{-3})	0.99 ± 0.27	0.71	1.41	0.66 ± 0.21	0.31	0.99
NO_3^--fine (μg m^{-3})	0.11 ± 0.07	0.04	0.26	0.18 ± 0.10	0.08	0.36
MSA-coarse	1.66 ± 0.78	0.92	3.00	2.15 ± 1.03	0.54	4.01
MSA-fine	24.79 ± 3.94	19.56	31.78	23.37 ± 8.16	11.77	28.03
NH_4^+-coarse	50.8 ± 22.3	11.8	84.3	31.7 ± 13.1	12.8	76.2
NH_4^+-fine	904 ± 248	566	1410	508 ± 238	232	1210
Na^+-coarse (μg m^{-3})	0.46 ± 0.14	0.19	0.64	0.52 ± 0.21	0.21	1.01
Na^+-fine (μg m^{-3})	0.35 ± 0.14	0.22	0.64	0.35 ± 0.15	0.13	0.65
K^+-coarse	34.0 ± 13.9	12.8	65.7	25.9 ± 12.4	11.1	65.7
K^+-fine	192 ± 58	105	277	139 ± 90	52.6	385
NSS-K^+-coarse	17.0 ± 10.5	5.9	42.1	6.63 ± 8.69	−8.00	4.21
NSS-K^+-fine	179.4 ± 56.2	96.5	253	125.7 ± 86.8	43.3	361
Mg^{2+}-coarse	63.7 ± 22.4	30.5	97.5	70.7 ± 31.2	24.2	131
Mg^{2+}-fine	44.0 ± 11.2	25.5	58.6	54.9 ± 17.4	31.1	88.2
NSS-Mg^{2+}-coarse	9.11 ± 11.75	−3.55	27.7	8.76 ± 19.80	−29.9	47.0
NSS-Mg^{2+}-fine	2.91 ± 13.4	−22.1	23.1	13.5 ± 12.9	−6.4	43.4
Ca^{2+}-coarse	257 ± 134	126	482	327 ± 184	59.1	705
Ca^{2+}-fine	72.0 ± 42.8	8.23	132	121 ± 69	56.2	300
NSS-Ca^{2+}-coarse	240 ± 131	111	459	307 ± 184	44.2	680
NSS-Ca^{2+}-fine	58.8 ± 41.5	−1.63	119	108.1 ± 69.1	43.1	288

[a]Sample number is 25 for the coarse, 26 for the fine fractions of the anions, and 27 for all cations. Concentrations are in ng m^{-3} unless otherwise noted.

present study, in the context of tracers for the distinct sources. More detailed trace metal data are presented in *Johansen and Hoffmann* [2003].

3. Results and Discussion

3.1. Air Mass Origins and Characteristics

[15] Air mass back trajectories for a number of samples are plotted in Figure 1. Trajectories and trace metal analysis [*Johansen and Hoffmann*, 2003] infer that the beginning of the cruise was characterized by air masses that originated over the Indian subcontinent, while conditions during the second half of the cruise were comparable to those encountered during the intermonsoon [*Johansen et al.*, 1999; *Siefert et al.*, 1999]. Therefore, samples IO97-01 through IO97-10 are classified as group 1 samples, with representative air mass back trajectories plotted in Figures 1a, 1b, and 1c, while samples IO97-11 through IO97-27 are classified as group 2 samples, with representative air mass back trajectories delineated in Figures 1d, 1e, 1f, 1g, and 1h. Group 1 samples have a larger anthropogenic component, seemingly originating from India, while group 2 samples contain appreciable amounts of mineral dust from the arid regions of Saudi Arabia.

3.2. Anions

[16] The average, minimum and maximum concentrations of the detected anions in coarse and fine fractions for both groups of samples are listed in Table 1. The non-sea-salt (NSS) concentrations of selected species are computed from their constant and known weight ratios with regard to Na^+ in sea-water, while assuming that Na^+ is a conservative sea-salt tracer.

[17] Relationships between anions, cations and 6 characteristic source trace metal tracers are analyzed with principal component (PC) analysis. The output of the Varimax rotated component matrix in Table 2 identifies correlations between chemical species and extracts their atmospheric sources. All tabulated components have eigenvalues larger than 1 and account for an accumulated variance of 91.0%. The first 4 components have real physical meaning, comparable to what we found in *Johansen and Hoffmann* [2003]. Component 1 accounts for 24.0% of the variance in the data and is characteristic of an anthropogenic component, high in Pb, Zn (especially in the fine fraction) and other combustion related products. The second component, accounting for 18.7% of the data's variance, displays typical crustal characteristics, high in coarse-Al, Ca, Mg, and Sc, while the third component (14.8% of variance) represents another crustal component, high in water-soluble Ca and Mg in the fine fraction. Water-soluble Ca and Mg have been observed in the atmosphere over the Indian Ocean in association with clay minerals in a previous study [*Johansen et al.*, 1999] as well as in other geographic regions [*Ali-Mohamed and Ali*, 2001; *Chung et al.*, 2001; *Satsangi et al.*, 2002; *Savoie and Prospero*, 1980]. Component 4 (9.8% of the variance) is the sea spray contribution, distinctly characterized by the large water-soluble Na and Cl contents in the coarse fraction. The next 4 components will be discussed below.

3.2.1. NSS-SO_4^{2-} and MSA

[18] Average total NSS-SO_4^{2-} concentrations observed during group 1 samples amounted to 3.84 ± 0.85 μg m^{-3} and during group 2 samples 2.45 ± 1.22 μg m^{-3}. Note the larger NSS-SO_4^{2-} concentration observed during the more polluted group 1 samples, suggesting a large anthro-

Table 2. Varimax Rotated Principal Component Martix[a]

	24.0%	18.7%	14.8%	9.8%	7.4%	6.7%	5.8%	3.7%
	1	2	3	4	5	6	7	8
Component Element	Anthrop.	Crustal	Crustal High in Ca and Mg	Sea Salt	Fine-Cl^--Def., An.-Cat.	Coarse-MSA, NSS-SO_4^{2-}	Fine-Cl^-, NO_3^-	Coarse-Cl^--Def., An.-Cat.
Al-coarse	0.028	**(0.957)**	0.024	0.081	0.010	0.079	−0.013	−0.004
Al-fine	−0.205	0.684	0.514	−0.137	−0.051	0.134	0.351	−0.026
Ca-coarse	−0.115	**(0.708)**	0.467	0.188	−0.013	−0.042	−0.104	0.340
Ca-fine	−0.074	0.114	**(0.909)**	0.011	−0.022	0.165	0.240	0.146
Mg-coarse	−0.191	**(0.886)**	0.198	0.241	0.037	0.010	0.022	0.114
Mg-fine	−0.217	0.458	**(0.755)**	0.006	−0.002	0.201	0.339	0.009
Sc-coarse	0.045	**(0.944)**	−0.077	0.070	0.023	0.104	−0.046	0.057
Sc-fine	−0.113	0.669	0.404	−0.382	−0.138	0.152	0.235	0.068
Zn-coarse	0.676	0.470	−0.171	0.066	0.114	0.154	−0.160	−0.143
Zn-fine	**(0.927)**	−0.040	−0.203	−0.004	0.027	0.151	0.102	−0.022
Pb-coarse	**(0.806)**	0.346	−0.086	0.162	−0.042	0.011	−0.158	−0.090
Pb-fine	**(0.932)**	−0.022	−0.022	0.116	−0.039	0.149	0.148	−0.005
Na^+-coarse	0.077	−0.013	0.093	**(0.945)**	0.165	0.050	0.021	0.151
Na^+-fine	0.157	0.008	0.213	0.432	**(0.821)**	0.064	0.094	−0.115
K^+-coarse	0.629	−0.029	−0.169	0.607	0.100	0.115	0.323	−0.015
K^+-fine	**(0.899)**	−0.160	−0.067	0.007	0.047	−0.143	−0.041	−0.247
NSS-K^+-coarse	**(0.754)**	−0.029	−0.276	0.181	0.024	0.116	0.397	−0.115
NSS-K^+-fine	**(0.897)**	−0.162	−0.082	−0.024	−0.012	−0.151	−0.049	−0.242
Mg^{2+}-coarse	0.088	0.508	0.130	0.771	0.129	0.135	0.144	−0.006
Mg^{2+}-fine	0.032	0.148	**(0.774)**	0.357	0.201	0.069	−0.129	−0.321
NSS-Mg^{2+}-coarse	0.044	**(0.813)**	0.090	0.049	−0.001	0.151	0.198	−0.197
NSS-Mg^{2+}-fine	−0.140	0.146	**(0.579)**	−0.101	−0.693	0.004	−0.238	−0.210
Ca^{2+}-coarse	−0.172	**(0.737)**	0.446	0.177	0.025	0.308	0.005	0.257
Ca^{2+}-fine	−0.163	0.116	**(0.945)**	0.056	0.120	0.049	0.039	0.120
NSS-Ca^{2+}-coarse	−0.176	**(0.744)**	0.446	0.138	0.018	0.308	0.004	0.252
NSS-Ca^{2+}-fine	−0.177	0.118	**(0.946)**	0.024	0.061	0.043	0.032	0.132
NH_4^+-coarse	0.428	−0.167	−0.380	0.036	−0.337	0.566	0.228	0.053
NH_4^+-fine	**(0.920)**	−0.137	−0.112	−0.186	0.086	−0.034	−0.184	0.136
Cl-coarse	−0.261	0.187	0.155	**(0.880)**	0.247	0.062	0.144	−0.049
Cl^--fine	−0.234	0.031	0.444	0.301	0.142	−0.221	**(0.702)**	−0.025
Cl^--deficit-coarse	**(0.661)**	−0.397	−0.141	−0.051	−0.195	−0.034	−0.247	**(0.371)**
Cl^--deficit-fine	0.262	−0.003	0.056	0.349	**(0.835)**	0.155	−0.173	−0.114
SO_4^{2-}-coarse	0.170	0.251	0.238	0.457	0.100	**(0.779)**	−0.083	0.054
SO_4^{2-}-fine	**(0.933)**	−0.161	0.040	−0.055	0.030	0.005	−0.273	0.077
NSS-SO_4^{2-}-coarse	0.159	0.301	0.229	0.027	0.028	**(0.888)**	−0.110	−0.017
NSS-SO_4^{2-}-fine	**(0.932)**	−0.161	0.034	−0.070	0.004	0.002	−0.277	0.081
NO_3^--coarse	**(0.691)**	0.403	−0.248	0.250	−0.120	0.255	−0.190	0.021
NO_3^--fine	−0.363	0.409	0.157	0.164	0.087	0.049	**(0.720)**	0.179
MSA-coarse	−0.210	0.346	0.149	−0.020	0.270	**(0.663)**	0.059	−0.053
MSA-fine	0.327	0.408	−0.223	**(0.435)**	0.031	0.064	−0.364	0.052
(Cat.-An.)-coarse	−0.168	0.274	0.216	0.098	−0.177	0.001	0.078	**(0.778)**
(Cat.-An.)-fine	−0.320	0.063	0.138	−0.014	**(0.861)**	0.015	0.097	−0.098

[a]Rotation converged in seven interations. Includes 23 samples. All components have eigenvalues >1 and account for a cumulative variance of 91.0%.

pogenic component. Total NSS-SO_4^{2-} values are in good agreement with those determined in a number of studies carried out during similar seasonal conditions [*Ball et al.*, 2003; *Clarke et al.*, 2002; *Gabriel et al.*, 2002; *Venkataraman et al.*, 2002]. Compared to the intermonsoons or SW monsoons, the present concentrations are larger by factors of about to 2 and 4, respectively [*Johansen et al.*, 1999].

[19] Most of the NSS-SO_4^{2-} (see Figure 2a) is in the fine fraction, 94.0% and 92.6%, for group 1 and group 2 samples, respectively. The sea-salt SO_4^{2-} contribution overall is small, on average 6.6%, and even less (<3%) when only considering the fine fraction.

[20] Methanesulfonic acid (CH_3SO_3H, MSA) is an oxidation product [*Hynes et al.*, 1986; *Yin et al.*, 1986] of dimethyl sulfide (CH_3SCH_3, DMS), which is the primary organosulfur compound emitted to the atmosphere [*Bates et al.*, 1992]. Average total MSA concentrations amount to 26.4 ± 4.3 ng m^{-3} and 25.4 ± 8.3 ng m^{-3} for samples in groups 1 and 2, respectively. These values are very close to what we observed over the Arabian Sea during the intermonsoon of 1995 [*Johansen et al.*, 1999]. MSA in the coarse and fine fractions is plotted in Figure 2b. The fine fraction accounts for 93.9 and 92.0% of the total MSA in groups 1 and 2 samples, respectively. This trend has been observed by a series of investigators [*Johansen et al.*, 2000; *Kerminen et al.*, 1997; *O'Dowd et al.*, 1997; *Pszenny*, 1992; *Qian and Ishizaka*, 1993; *Quinn et al.*, 1993] and is presumably a function of the surface area of the sea-salt aerosol.

3.2.2. NSS-SO_4^{2-} Source Apportionment

[21] NSS-SO_4^{2-} can have anthropogenic, biogenic, and crustal sources, which magnitudes cannot be directly measured, but are of considerable interest within the topic of global climate and biogeochemical cycles. One way of estimating the relative contribution of each source is by finding appropriate proxies (an element or a compound that varies linearly in proportion to the given SO_4^{2-} source) and performing weighted multivariate linear least squares regression analyses [*Johansen et al.*, 1999].

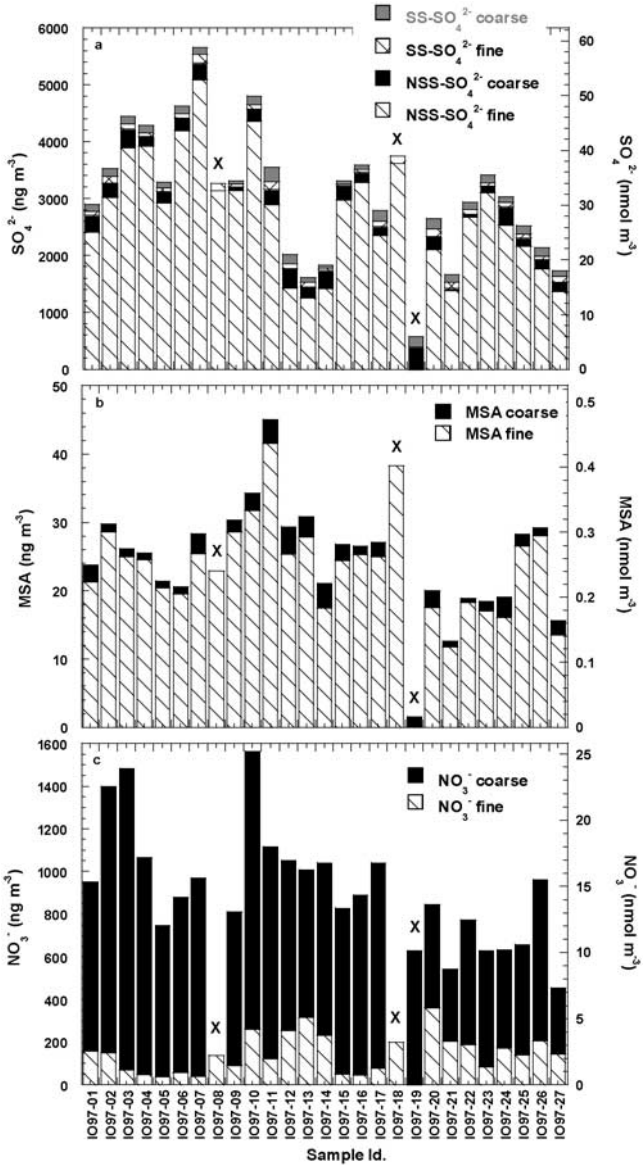

Figure 2. (a) SS- and NSS-SO_4^{2-}, (b) MSA, and (c) NO_3^- concentrations in coarse and fine aerosol fractions versus sample ID.

[22] The PC analysis in Table 2 can be of some help in choosing the right proxies. The anthropogenic component, PC 1, indicates that Pb, Zn, NH_4^+, or NSS-K^+ could be used as proxy for the fine NSS-SO_4^{2-} fraction. On the other hand, the coarse NSS-SO_4^{2-} seems to be solely represented by PC 6, which correlates with MSA in the coarse fraction. MSA and SO_4^{2-} are oxidation products from the initial reaction of DMS with hydroxy radical ($OH^\bullet$) and nitrate radical ($NO_3^\bullet$), and because their relative yields is determined by temperature [*Hynes et al.*, 1986] MSA is considered a quasi-conservative tracer for the marine biogenic NSS-SO_4^{2-} component. The crustal SO_4^{2-} source does not seem to be very strong, but shows up in PC 2 and PC 3, in the form of NSS-Ca^{2+}, or NSS-Mg^{2+}.

[23] Linear regression analyses were performed on coarse and fine fractions separately. From a large number of combinations of proxies as well as different grouping of the samples, the best model outputs are presented in Table 3, the first two for the coarse and the second two for the fine fractions.

[24] The goodness of fit can be established by a number of factors: the analysis of variance (ANOVA) output of the model, the coefficient for Na^+ (the SO_4^{2-}/Na^+ ratio in sea-water is 0.2516), and the magnitude of the constant (intercept). In the first three models the dependent variable was chosen to be SO_4^{2-} rather than NSS-SO_4^{2-} in order to be able to use the coefficient for SS-SO_4^{2-} to assess the model.

[25] The only difference between the first and second models for the coarse fraction is that that second model was forced through the origin, which is justifiable based on the 62.2% significance of the null-hypothesis for the constant in the first model. All but one parameter, the SS-SO_4^{2-}/Na^+ ratio, seem to indicate that the second model is a better fit. Based on the latter model the bio-SO_4^{2-}/MSA ratio becomes 52.8, with 95% confidence intervals extending from 24.7 to 80.8. This value, including the confidence interval, is higher than expected based on observations from remote parts of the open ocean, where anthropogenic and crustal contributions were assumed to be negligible and values close to 14 or 15 were observed [*Bürgermeister and Georgii*, 1991; *Gao et al.*, 1996; *Johansen et al.*, 1999; *Saltzman et al.*, 1985, 1983; *Savoie and Prospero*, 1989, 1994]. *Savoie et al.* [2002] used a modified linear regression analysis to find a biogenic ratio of 19.6 (95% C.I. 19.4–19.8) in Barbados. Based on *Johansen et al.*'s [1999] temperature dependence for this ratio and a mean temperature of 25.3 °C observed during the present cruise, an overall bio-SO_4^{2-}/MSA weight ratio of 9 to 10 is predicted.

[26] A number of potential factors may be contributing to the unexpectedly large bio-SO_4^{2-}/MSA ratio. Unlike in the other studies, coarse and fine fractions were here collected separately. According to *Kerminen et al.* [1997] the mass size distribution for MSA peaks at slightly smaller size than NSS-SO_4^{2-}, which is potentially brought about by evaporation and recondensation of MSA. Such redistribution of MSA into, in our experiment, the fine mode (<3 μm) would lead to larger bio-SO_4^{2-}/MSA ratios in our coarse mode. Furthermore, one needs to keep in mind that the ratio of two small numbers, MSA and NSS-SO_4^{2-} concentrations in the coarse mode, is susceptible to large errors.

[27] As is, the magnitudes of the standardized coefficients in model 1 in Table 3 give a measure of the relative contribution of each of the components. Thus, about 40% of the coarse SO_4^{2-} is sea-salt derived, 30% is of biogenic and 30% of anthropogenic nature.

[28] The third and fourth model outputs in Table 3 are for the fine fraction SO_4^{2-} and NSS-SO_4^{2-}, respectively. In considering the goodness of the fits, neither of these models could be considered completely satisfactory in extracting a biogenic SO_4^{2-}/MSA ratio. The null-hypothesis for MSA is almost 30% in both cases and the constant is not insignificant. However, in considering the fourth model, 84.3% of NSS-SO_4^{2-} would be of anthropogenic, 5.6% of biogenic, and 10.1% of crustal origin. Although the observed biogenic SO_4^{2-}/MSA ratio of 9.8 is exactly what would be expected (vide supra), the 95% confidence interval extends from −9.1 to 28.7. It is clear that MSA in the fine fraction is subject to a more complex picture compared to MSA in the coarse

Table 3. Weighted Multiple Linear Least Squares Regression Outputs for Coarse and Fine SO_4^{2-} Fractions as Dependent Variable

Dependent Variable	Model Summary			Independent Variables	Unstandardized Coefficients		Standardized Coefficients			95% Confidence Interval for B	
	R^2	F	Sig.		B	Std. Error	b	t	Sig.	Lower Bound	Upper Bound
coarse-SO_4^{2-}	0.583	9.803	0.000	(constant)	31.418	62.770		0.501	0.622	−99.119	161.955
				Na^+-coarse	0.253	0.081	0.450	3.112	0.005	0.084	0.422
				MSA-coarse	49.216	15.476	0.451	3.180	0.005	17.032	81.400
				NO_3^--coarse	0.112	0.054	0.298	2.066	0.051	−0.001	0.226
coarse-SO_4^{2-}	0.966	208.952	0.000	Na^+-coarse	0.272	0.071	0.406	3.851	0.001	0.126	0.418
				MSA-coarse	52.753	13.532	0.320	3.899	0.001	24.691	80.816
				NO_3^--coarse	0.128	0.043	0.298	2.953	0.007	0.038	0.218
fine-SO_4^{2-}	0.930	70.124	0.000	(constant)	355.619	295.541		1.203	0.242	−258.992	970.230
				Na^{2+}-fine	0.071	0.458	0.010	0.155	0.878	−0.881	1.023
				MSA-fine	10.800	9.594	0.071	1.126	0.273	−9.151	30.752
				NH_4^+-fine	3.246	0.215	0.978	15.113	0.000	2.800	3.693
				NSS-Ca^{2+}-fine	1.952	1.018	0.123	1.917	0.069	−0.166	4.069
fine-NSS-SO_4^{2-}	0.929	95.468	0.000	(constant)	338.441	286.953		1.179	0.251	−256.664	933.546
				MSA-fine	9.808	9.096	0.065	1.078	0.293	−9.056	28.672
				NH_4^+-fine	3.229	0.205	0.980	15.728	0.000	2.803	3.655
				NSS-Ca^{2+}-fine	1.864	0.975	0.118	1.911	0.069	−0.159	3.887

fraction and to what we found during the intermonsoons and SW monsoons of 1995 [*Johansen et al.*, 1999]. Possible mechanisms that may contribute to this complexity are the evaporation and redeposition of MSA onto fine aerosols with higher area/volume ratios, a process which in turn will depend on the particles pH, and the fractionation of components in the submicrometer size range particles as a result of bubble bursting and subsequent fragmentation [*Katoshevski*, 2001; *Nilsson et al.*, 2001]. Furthermore, temperature fluctuations between days and within a day were considerable and may contribute to the difficulty in extracting a constant for the ratio.

3.2.3. NO_3^-

[29] Total NO_3^- averages 1.10 ± 0.31 μg m^{-3} during group 1 samples and 0.79 ± 0.33 μg m^{-3} during group 2 samples. *Savoie et al.* [1987] reported NO_3^- aerosol concentrations over the Arabian Sea that are smaller by a factor of 2 (0.43 ± 0.34 μg m^{-3}) compared to those observed herein. However, their values for NSS-SO_4^{2-} and mineral aerosol were also small compared to our observations and those reported by other investigators. *Naik et al.* [1991] measured ~2.5 μg m^{-3} of NO_3^- during the month of May of 1983, while we [*Johansen et al.*, 1999] detected 1.23 ± 0.41 μg m^{-3} during May of 1995. Nitrate concentrations dropped to 0.46 ± 0.12 μg m^{-3} during the SW-monsoon [*Johansen et al.*, 1999]. *Rhoads et al.* [1997] found NO_3^- concentrations of 2.68 ± 0.95 μg m^{-3} during the months of March and April of 1995.

[30] NO_3^- concentrations in coarse and fine fractions are plotted in Figure 2c as a function of sample ID. In contrast to other anthropogenically derived species, such as Zn, Pb and NH_4^+, NO_3^- is found more abundant (90.0% in group 1 and 83.3% in group 2 samples) in the coarse fraction. This observation is in agreement with those made by other investigators [*Berresheim et al.*, 1991; *Huebert et al.*, 1996; *Johansen et al.*, 2000; *Naik et al.*, 1991; *Savoie and Prospero*, 1982; *Sievering et al.*, 1990]. The reason is that in temperate regions and in the presence of H_2SO_4 [*Bassett and Seinfeld*, 1984; *Sisterson*, 1989], HNO_3 evaporates from small particles and is subsequently deposited on large particles, which may be marine- or soil-derived. The PC analysis supports this phenomenon by demonstrating that NO_3^- in the coarse fraction correlates with the anthropogenic component. On the other hand, the fine fraction NO_3^- correlates with the fine Cl^- in PC 7.

3.2.4. Cl^-

[31] All Cl^- concentrations are below the expected values from the sea-salt contained in the samples as traced by Na^+. The relative deficit (%Cl^- deficit = (SS-Cl^- - observed-Cl^-)/SS-Cl^-) for coarse and fine fractions is plotted in Figure 3a. In the coarse fraction the deficit is $46.5 \pm 15.5\%$ in group 1 and $25.0 \pm 23.9\%$ in group 2 samples, while in the fine fraction the corresponding numbers are $96.0 \pm 3.9\%$ and $86.0 \pm 19.1\%$. The deficit is considerably larger than observed previously by our group over the Arabian Sea [*Johansen et al.*, 1999] during the SW- and intermonsoons. The Cl^- deficits during those cruises were $3.5 \pm 6.3\%$ and $15 \pm 9\%$, respectively. Over the tropical Atlantic Ocean [*Johansen et al.*, 2000] we measured Cl^- deficits of $11.9 \pm 13.3\%$ in the coarse fraction and $29.7 \pm 9.9\%$ in the fine fraction. Chloride deficits have been found to correlate with the proximity to continental landmasses, and thus are assumed to depend on the concentrations of anthropogenic pollutants such as SO_4^{2-} and NO_3^-. In heavily polluted air masses, losses of particulate Cl^- approaching 100% have been reported. Based on these observations, it is assumed that Cl^- is released solely due to the thermodynamically favorable displacement reactions between mineral acids (H_2SO_4, HNO_3) and HCl:

$$2\ NaCl(s) + H_2SO_4 \rightarrow Na_2SO_4 + 2\ HCl(g) \quad (1)$$

$$NaCl(s) + HNO_3 \rightarrow NaNO_3 + HCl(g). \quad (2)$$

Recent investigations provide evidence that in addition to HCl, highly reactive Cl gases such as Cl_2, HOCl, $ClNO_2$, and BrCl may also volatilize from sea-salt aerosol [*Fan and Jacob*, 1992; *Graedel and Keene*, 1995, 1996; *Langer et al.*, 1996; *Sander and Crutzen*, 1996; *Vogt et al.*, 1996].

[32] Paring earlier cruises [*Johansen et al.*, 1999, 2000] we found evidence for the release of Cl from the aerosol phase by both mechanisms. From the PC analysis given in Table 2, the Cl^- deficit in the coarse fraction correlates with the anthropogenic component (PC 1) which also correlates with NO_3^- in the coarse fraction. The Cl^- deficit in the

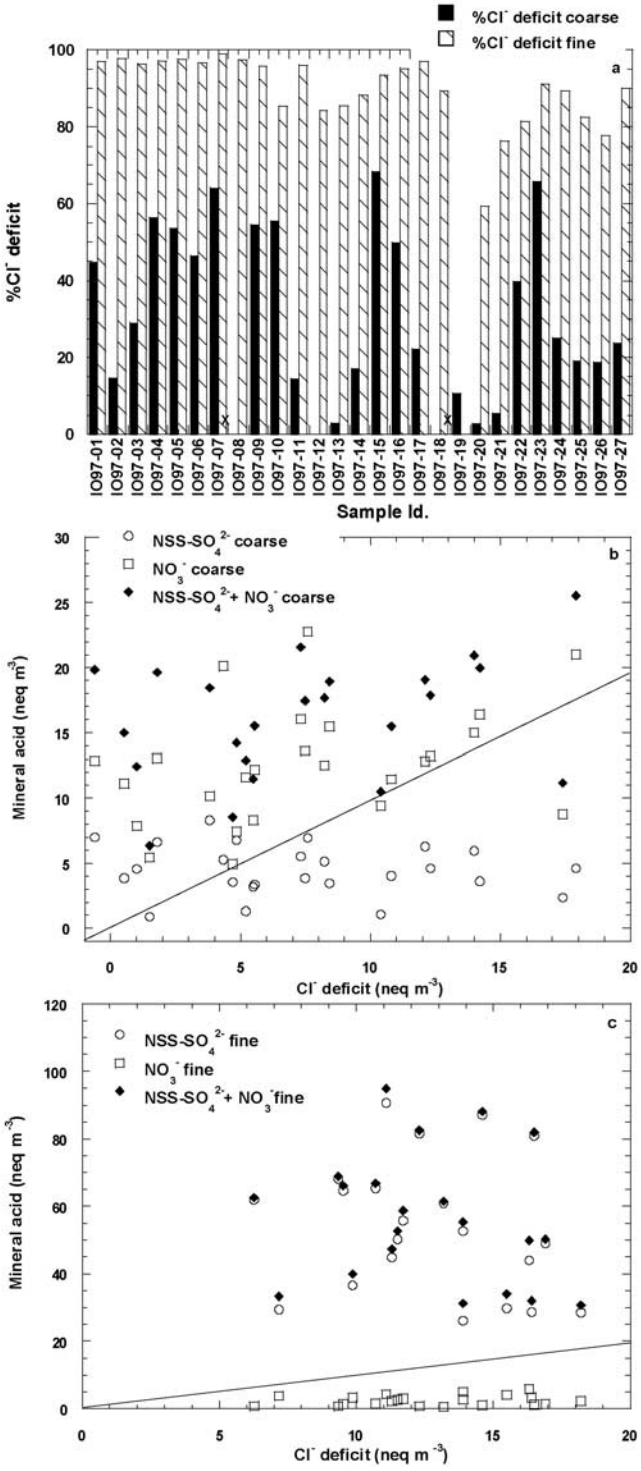

Figure 3. (a) Percent Cl^- deficit in coarse and fine fractions versus sample ID. Mineral acid concentrations versus Cl^- deficit in (b) coarse and (c) fine fraction. The line is representative of conditions when mineral acid concentrations equal Cl^- deficit.

coarse fraction may be due to the acid displacement reaction with HNO_3. This process is further investigated in Figure 3b where concentrations of the mineral acids are plotted as a function of Cl^- deficit in the coarse fraction. The drawn 1:1 line represents data points for which the Cl^- deficit is exactly matched with the concentration of the specific mineral acid. Thus, points to the right of the line indicate that there is not enough of the particular mineral acid present to account for the Cl^- deficit found in the samples. In spite of the scatter there is a weak correlation between the NO_3^- and the Cl^- deficit (as noticed in the PC analysis), and 92% of the samples contain enough NO_3^- (positioned to the left of the 1:1 line) to account for the Cl^- deficit. This indicates that HNO_3 in the acid displacement reaction may be the most important contributor to C- deficit in the coarse fraction. This trend was also observed by *Sievering et al.* [1990]. However, it does not exclude the possibility that H_2SO_4 and/or the reactive Cl species may have contributed to the Cl^- deficit. In fact, there is an indication, from the weak correlation between the coarse Cl^- deficit and the surplus of cations (Cat.-An. chargers) in PC 8 that the alternative idea of the volatilization of reactive Cl is contributing to the deficit. When Cl is released in the form of reactive species the lost anionic charge may not be replaced by a detectable anion and may thus become traceable by the discrepancy between the cationic and anionic charges.

[33] The Cl^- deficit in the fine fraction in reference to the mineral acids is plotted in Figure 3c. This plot illustrates that the NO_3^- concentrations are not sufficient to account for the observed Cl^- deficit. But SO_4^{2-} is present in more than sufficient quantities, thus it may be the principal mineral acid affecting the displacement of Cl^- in the fine fraction. A correlation between Cl^- deficit and NSS-SO_4^{2-} in the fine fraction would strengthen the argument for this reaction, however, the NSS-SO_4^{2-} concentrations are large enough compared to the Cl^- deficit that this effect may be washed out. The possibility of Cl release in the fine fraction due to the production of reactive Cl species seems to be of significance due to the strong correlation between Cl^- deficit and surplus of cationic charges in PC 5.

3.3. Cations

[34] The observed cation concentrations are summarized in Table 1. Assuming that all the water-soluble Na^+ is sea-salt derived, the NSS contributions for the alkali and alkaline earth elements were determined based on seawater concentrations reported by *Millero and Sohn* [1992].

3.3.1. NH_4^+

[35] Total ammonium concentrations averaged 0.95 ± 0.25 μg m^{-3} and 0.54 ± 0.23 μg m^{-3} during group 1 and group 2 samples. Group 2 values are very close to those observed by *Rhoads et al.* [1997] over the Arabian Sea during March and April of 1995. During the intermonsoon of 1995, we observed values that were smaller by a factor of 2 compared to the Group 2 values, and during the SW-monsoon of the same year NH_4^+ concentrations were smaller by a factor of 15 [*Johansen et al.*, 1999]. Most (94.8% and 94.0%, group 1 and group 2, respectively) of the NH_4^+ is present in the fine fraction; this is reflected in Figure 4a. Ammonium has typically been observed in association with the accumulation mode, together with NSS-SO_4^{2-} and MSA [*Huebert et al.*, 1996; *Kerminen et al.*, 1997]. This concept is in agreement with our observations and is reaffirmed in the PC analysis presented in

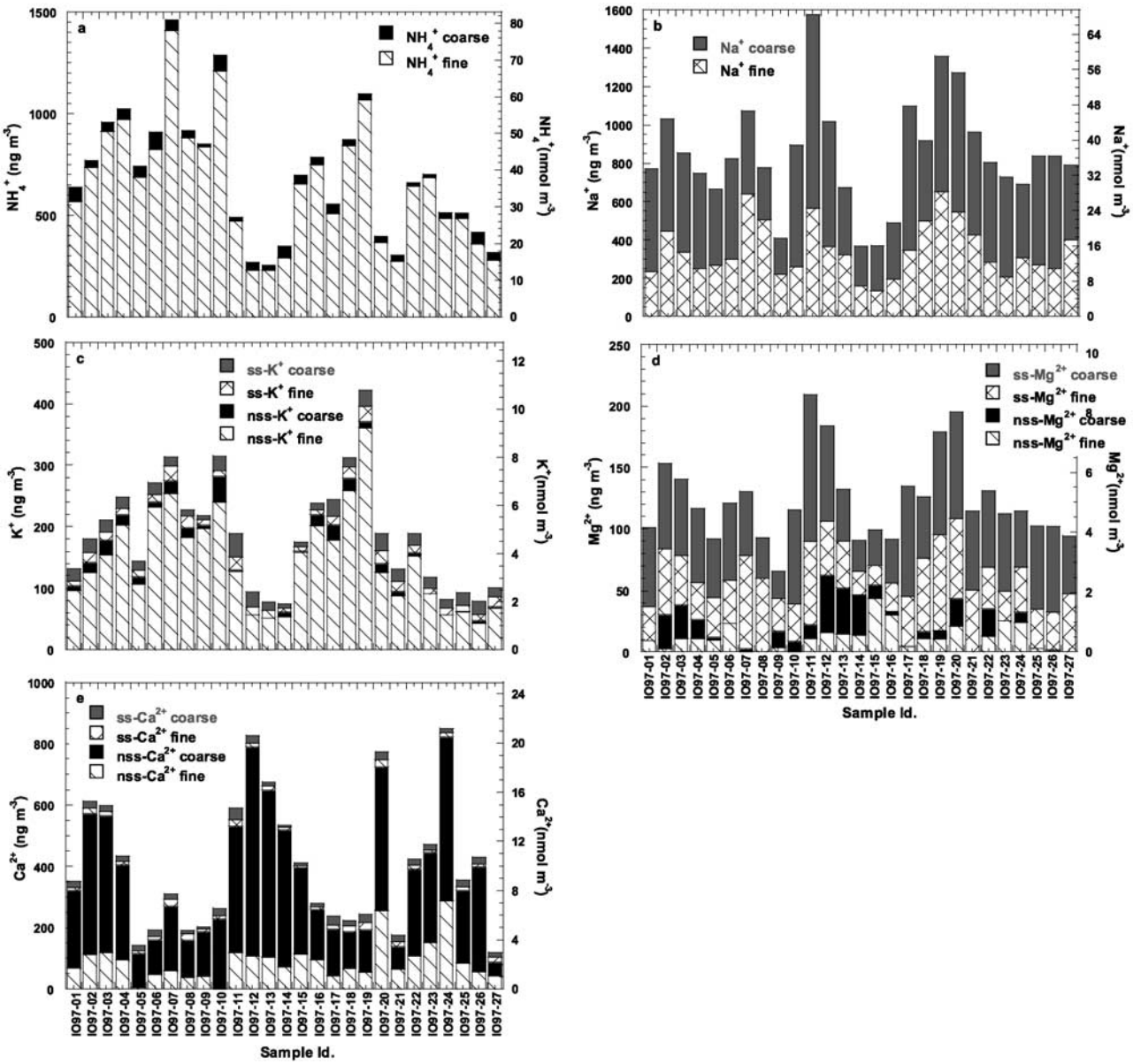

Figure 4. Cation concentrations in coarse and fine fractions versus sample ID: (a) NH_4^+, (b) Na^+, (c) SS- and NSS-K^+, (d) SS- and NSS-Mg^{2+}, and (e) SS- and NSS-Ca^{2+}.

Table 2. Ammonium ion in these samples appears to be of anthropogenic origin.

3.3.2. Na^+, K^+, Mg^{2+}, and Ca^{2+}

[36] Total Na^+ concentrations of 0.80 ± 0.19 μg m^{-3} and 0.87 ± 0.33 μg m^{-3} were determined in group 1 and group 2 samples, respectively. *Rhoads et al.* [1997] and *Savoie et al.* [1987] observed slightly higher Na^+ concentrations over the Arabian Sea, 1.11 ± 0.44 and 2.4 ± 1.2 μg m^{-3}, respectively. During the intermonsoon and SW monsoon of 1995 [*Johansen et al.*, 1999], we also observed larger values, 2.6 ± 1.4 and 6.5 ± 2.9 μg m^{-3}, respectively. Due to the relatively low wind speeds encountered in the present cruise the sea-salt loading is on average evenly distributed in the coarse and fine fractions. This is discernible in Figure 4b, which shows Na^+ in coarse and fine fractions.

[37] NSS and SS contributions (using Na^+ as the sea-salt tracer) of water-soluble K^+ in both coarse and fine fractions are plotted in stacked bars of Figure 4c. The K^+ signature is very similar to that in the plot above, for the anthropogenic NH_4^+. Analogously with NH_4^+, most of the K^+ is found in the fine fraction (85.0% and 84.2% in group 1 and group 2 samples, respectively), of which 93.2% and 90.6% is NSS-K^+ fine, in agreement with *Ball et al.*'s [2003] findings during INDOEX. K is released in the combustion of vegetation, wood and from waste incinerators [*Andreae*, 1983; *Echalar et al.*, 1995; *Fishman et al.*, 1999]. During the intermonsoon of 1995 [*Johansen et al.*, 1999], when some of the air masses appear to have similar origins as during group 2 samples of the present cruise, the K^+ concentrations averaged $0.18 \pm .11$ μg m^{-3} of which $40.8 \pm 16.0\%$ were NSS. While the total K^+ concentrations are in general agreement, the contribution in the NSS fraction is much lower during the intermonsoon. This is an indication that group 2 samples are also

influenced by polluted air masses from the Indian subcontinent. K^+ and NSS-K^+ concentrations reported from INDOEX [*Ball et al.*, 2003; *Gabriel et al.*, 2002] are in agreement with presently reported values.

[38] Mg^{2+} NSS and SS contributions in the coarse and fine fractions are plotted in Figure 4d, analogously with the K plot. The Mg^{2+} NSS contributions account for, on average, only 11.1% and 17.6% of the total Mg^{2+}, in group 1 and group 2 samples, respectively. While 75.9% of this NSS-Mg^{2+} is in the coarse fraction for group 1 samples, only 39.5% is in the coarse fraction in group 2 samples. Assuming this NSS-Mg^{2+} is of crustal origin, this shows that two crustal sources, high in water-soluble Mg, and distinguished by their particle size, contribute to the aerosol mass during the present cruise.

[39] Associated with the crustal Mg^{2+} is also a Ca^{2+} component (PC 3 in Table 2), potentially derived from calcite/gypsum/limestone/dolomite. The plot in Figure 4e reflects a much larger relative NSS contribution in Ca^{2+} than in Mg^{2+}. On average, 90.9% and 92.6% of the Ca^{2+} is NSS, whereby 80.3% and 74.7% of this NSS-Ca^{2+} is present in the fine fractions of group 1 and group 2 samples, respectively. During the intermonsoon of 1995 [*Johansen et al.*, 1999] the NSS-Ca^{2+} averaged 0.96 ± 0.90 μg m^{-3} and seemed to be attributed mainly to gypsum. This value is more than twice that observed during group 2 samples (0.42 ± 0.23 μg m^{-3}) from the present cruise.

4. Conclusions

[40] All atmospheric aerosol samples collected during the month of March of 1997 over the Arabian Sea carry a strong anthropogenic signature reflected in the large enrichments in anthropogenic tracers such as Pb, Zn, fine K, NSS-K^+, NSS-SO_4^{2-}, NH_4^+, and coarse NO_3^-. Since the anthropogenic contribution is especially pronounced in the first 10 samples, exhibiting air mass back trajectories that indicate a northeastern origin, these samples are collectively analyzed (group 1 samples) and discussed in reference to the collection of remaining samples (group 2 samples).

[41] NSS-SO_4^{2-} concentrations vary from 1.42 to 5.38 μg m^{-3} and average 2.94 ± 1.06 μg m^{-3}. This corresponds to $92.7 \pm 3.4\%$ of the total SO_4^{2-}. Most of the NSS-SO_4^{2-} ($92.1 \pm 4.5\%$) is present in the fine fraction and is associated with other anthropogenic tracers. Multiple linear regression analyses using MSA as the biogenic tracer and a number of different anthropogenic tracers to model SO_4^{2-} source apportionment revealed that in the fine fraction potential complex physical processes, possibly involving evaporation and redeposition of MSA, obscure the analyses. However, most of the NSS-SO_4^{2-} in the fine fraction seems of anthropogenic nature, with the biogenic component contributing only about 6% and the crustal component 10%. In the coarse fraction, however, 50% of the NSS-SO_4^{2-} seems to be biogenically and the other half anthropogenically derived. The NSS-SO_4^{2-}/MSA ratio in the coarse fraction of 52.8 (95% confidence interval = 24.7–80.8), is significantly larger than expected based on reported values.

[42] Cl^- deficits are observed in all the samples. They average $53.1 \pm 16.0\%$ of the expected Cl^- concentrations. In the fine fraction, however, Cl^- deficits up to 99.1% are found (average, $89.0 \pm 9.4\%$). Acid displacement reactions with H_2SO_4 may be responsible for the volatilization of HCl in the fine fraction, since the NSS-SO_4^{2-} concentrations are much larger than the displaced Cl^-, but the release of Cl^- from the particle phase by mechanisms such as the production of reactive Cl species seems to contribute considerably based on the charge deficit. In the coarse fraction acid displacement with HNO_3 seems the most predominant mechanism for the Cl^- deficit, which the production of reactive Cl species being secondary.

[43] **Acknowledgments.** This work is abstracted in part from the Ph.D. thesis of A. M. Johansen, California Institute of Technology. The authors wish to thank Drs. Meinrat O. Andreae and Hermann W. Bange (latter, now at Center for Marine Science, Kiel, Germany) from the Max Planck Institute of Biogeochemistry in Mainz, Germany, for assistance with the cruise, which was sponsored by the German Joint Global Ocean Flux Study (JGOFS) project. Appreciation is also extended to the helpful crew of the R/V *Sonne*. Research support was provided by the National Science Foundation and by the Environmental Now Foundation. Their support is greatly appreciated.

References

Ackerman, A. S., and S. K. Cox (1989), Surface weather observations of atmospheric dust over the southwest summer monsoon region, *Meteorol. Atmos. Phys.*, *41*, 19–34.

Ali-Mohamed, A. Y., and H. A. N. Ali (2001), Estimation of atmospheric inorganic water-soluble particulate matter in Muharraq Island, Bahrain, (Arabian Gulf), by ion chromatography, *Atmos. Environ.*, *35*(4), 761–768.

Andreae, M. O. (1983), Soot carbon and excess fine potassium: Long-range transport of combustion-derived aerosols, *Science*, *220*, 1148–1151.

Ball, W. P., R. R. Dickerson, B. G. Doddridge, J. W. Stehr, T. L. Miller, D. L. Savoie, and T. P. Carsey (2003), Bulk and size-segregated aerosol composition observed during INDOEX 1999: Overview of meteorology and continental impacts, *J. Geophys. Res.*, *108*(D10), 8001, doi:10.1029/2002JD002467.

Bassett, M. E., and J. H. Seinfeld (1984), Atmospheric equilibrium model of sulfate and nitrate aerosols, II, Particle size analysis, *Atmos. Environ.*, *18*(6), 1163–1170.

Bates, T. S., J. A. Calhoun, and P. K. Quinn (1992), Variations in the methanesulfonate to sulfate molar ratio in submicrometer marine aerosol particles over the South Pacific Ocean, *J. Geophys. Res.*, *97*, 9859–9865.

Berresheim, H., M. O. Andreae, R. L. Iverson, and S. M. Li (1991), Seasonal variations of dimethylsulfide emissions and atmospheric sulfur and nitrogen species over the western North Atlantic Ocean, *Tellus, Ser. B*, *43*, 353–372.

Berresheim, H., P. Wine, and D. Davis (1995), Sulfur in the atmosphere, in *Composition, Chemistry, and Climate of the Atmosphere*, edited by H. Singh, pp. 251–307, Van Nostrand Reinhold, New York.

Bürgermeister, S., and H.-W. Georgii (1991), Distribution of methanesulfonate, nss-sulfate and dimethylsulfide over the Atlantic and the North Sea, *Atmos. Environ., Part A*, *25*(3/4), 587–595.

Chand, D., S. Lal, and M. Naja (2003), Variations of ozone in the marine boundary layer over the Arabian Sea and the Indian Ocean during the 1998 and 1999 INDOEX campaigns, *J. Geophys. Res.*, *108*(D6), 4190, doi:10.1029/2001JD001589.

Charlson, R. J., J. E. Lovelock, M. O. Andreae, and S. G. Warren (1987), Oceanic phytoplankton, atmospheric sulphur, cloud albedo and climate, *Nature*, *326*, 655–661.

Chung, A., J. D. Herner, and M. J. Kleeman (2001), Detection of alkaline ultrafine atmospheric particles at Bakersfield, California, *Environ. Sci. Technol.*, *35*(11), 284–290.

Clarke, A. D., et al. (2002), INDOEX aerosol: A comparison and summary of chemical, microphysical, and optical properties observed from land, ship, and aircraft, *J. Geophys. Res.*, *107*(D19), 8033, doi:10.1029/2001JD000572.

Echalar, F., A. Gaudichet, H. Cachier, and P. Artaxo (1995), Aerosol emissions by tropical forest and savanna biomass burning: Characteristic trace elements and fluxes, *Geophys. Res. Lett.*, *22*(22), 3039–3042.

Eldering, A., J. A. Ogren, Z. Chowdhury, L. S. Hughes, and G. R. Cass (2002), Aerosol optical properties during INDOEX based on measured aerosol particle size and composition, *J. Geophys. Res.*, *107*(D22), 8001, doi:10.1029/2001JD001572.

Fan, S.-M., and D. J. Jacob (1992), Surface ozone depletion in Arctic spring sustained by bromine reactions on aerosol, *Nature*, *359*, 522–524.

Findlater, J. (1969), A major low-level air current near the Indian Ocean during the northern summer, *Q. J. R. Meteorol. Soc.*, *95*, 362–380.

Findlater, J. (1971), Mean monthly airflow at low levels over the western Indian Ocean, *Geophys. Mem.*, *115*, 1–53.

Finlayson-Pitts, B. J., M. J. Ezell, and J. N. Pitts Jr. (1989), Formation of chemically active chlorine compounds by reactions of atmospheric NaCl particles with gaseous N_2O_5 and $ClONO_2$, *Nature*, *337*, 241–244.

Fishman, N. S., C. A. Rice, G. N. Breit, and R. D. Johnson (1999), Sulfur-bearing coatings in fly ash from a coal-fired power plant: Composition, origin, and influence on ash alteration, *Fuel*, *78*, 187–196.

Gabriel, R., O. L. Mayol-Bracero, and M. O. Andreae (2002), Chemical characterization of submicron aerosol particles collected over the Indian Ocean, *J. Geophys. Res.*, *107*(D19), 8005, doi:10.1029/2000JD000034.

Gao, Y., R. Arimoto, R. A. Duce, L. Q. Chen, M. Y. Zhou, and D. Y. Gu (1996), Atmospheric non-sea-salt sulfate, nitrate, and methanesulfonate over the China Sea, *J. Geophys. Res.*, *101*, 12,601–12,611.

Graedel, T. E., and W. C. Keene (1995), Tropospheric budget of reactive chlorine, *Global Biogeochem. Cycles*, *9*(1), 47–77.

Graedel, T. E., and W. C. Keene (1996), The budget and cycle of Earth's natural chlorine, *Pure Appl. Chem.*, *68*(9), 1689–1697.

Huebert, B. J., L. Zhuang, S. Howell, K. Noone, and B. Noone (1996), Sulfate, nitrate, methanesulfonate, chloride, ammonium, and sodium measurements from ship, island, island, and aircraft during the Atlantic Stratocumulus Transition Experiment/Marine Aerosol Gas Exchange, *J. Geophys. Res.*, *101*, 4413–4423.

Hynes, A. J., P. H. Wine, and D. H. Semmes (1986), Kinetics and mechanism of OH reactions with organic sulfides, *J. Phys. Chem.*, *90*, 4148–4156.

Johansen, A. M., and M. R. Hoffmann (2003), Chemical characterization of ambient aerosol collected during the northeast-monsoon season over the Arabian Sea: Labile Fe(II) and other trace metals, *J. Geophys. Res.*, *108*(D14), 4408, doi:10.1029/2002JD003280.

Johansen, A. M., R. L. Siefert, and M. R. Hoffmann (1999), Chemical characterization of ambient aerosol collected during the southwest-monsoon and intermonsoon seasons over the Arabian Sea: Anions and cations, *J. Geophys. Res.*, *104*, 26,325–26,347.

Johansen, A. M., R. L. Siefert, and M. R. Hoffmann (2000), Chemical composition of aerosols collected over the tropical North Atlantic Ocean, *J. Geophys. Res.*, *105*, 15,277–15,312.

Katoshevski, D. (2001), Analysis of a sea spray: Effect of simultaneous growth and fragmentation on droplet/particle size distribution of a multi-component aerosol, *Atomization Sprays*, *11*(6), 643–652.

Keene, W. C., A. A. P. Pszenny, D. J. Jacob, R. A. Duce, J. N. Galloway, J. J. Schultz-Tokos, H. Sievering, and J. F. Boatman (1990), Geochemical cycling of reactive chlorine through the marine troposphere, *Global Biogeochem. Cycles*, *4*(4), 407–430.

Keene, W. C., D. J. Jacob, and S.-M. Fan (1996), New directions: Reactive chlorine—A potential sink for dimethylsulfide and hydrocarbons in the marine boundary layer, *Atmos. Environ.*, *30*(6), 1–3.

Keene, W. C., R. Sander, A. A. P. Pszenny, R. Vogt, P. J. Crutzen, and J. N. Galloway (1998), Aerosol pH in the marine boundary layer: A review and model evaluation, *J. Aerosol Sci.*, *29*(3), 339–356.

Kerminen, V.-M., M. Aurela, R. E. Hillamo, and A. Virkkula (1997), Formation of particulate MSA: Deductions from size distribution measurements in the Finnish Arctic, *Tellus, Ser. B*, *49*, 159–171.

Kottmeier, C., and B. Fay (1998), Trajectories in the Antarctic lower troposphere, *J. Geophys. Res.*, *103*(D9), 10,947–10,959.

Langer, S., B. T. McGovney, B. J. Finlayson-Pitts, and R. M. Moore (1996), The dimethyl sulfide reaction with atomic chlorine and its implications for the budget of methyl chloride, *Geophys. Res. Lett.*, *23*(13), 1661–1664.

McInnes, L. M., D. S. Covert, P. K. Quinn, and M. S. Germani (1994), Measurements of chloride depletion and sulfur enrichment in individual sea-salt particles collected from the remote marine boundary layer, *J. Geophys. Res.*, *99*, 8257–8268.

Middleton, N. J. (1986a), Dust storms in the Middle East, *J. Arid Environ.*, *10*, 83–96.

Middleton, N. J. (1986b), A geography of dust storms in southwest Asia, *J. Climatol.*, *6*, 83–96.

Millero, F. J., and M. L. Sohn (1992), *Chemical Oceanography*, CRC Press, Boca Raton, Fla.

Naik, M. S., L. T. Khemani, G. A. Momin, and P. D. Safai (1991), Origin of calcium in marine aerosol over the Arabian Sea near the west coast of India, *J. Aerosol Sci.*, *22*(3), 365–372.

Nair, P., R. Rajan, K. Parameswaran, A. Abraham, and S. Jacob (2001), Chemical composition of aerosol particles over the Arabian Sea and the Indian Ocean regions during the INDOEX (FFP-98) cruise—Preliminary results, *Curr. Sci.*, *80*, 171–175.

Nilsson, E. D., U. Rannik, E. Swietlicki, C. Leck, P. P. Aalto, J. Zhou, and M. Norman (2001), Turbulent aerosol fluxes over the Arctic Ocean: 2. Wind-driven sources from the sea, *J. Geophys. Res.*, *106*(D23), 32,139–32,154.

Norman, M., C. Leck, and H. Rodhe (2003), Differences across the ITCZ in the chemical characteristics of the Indian Ocean MBL aerosol during INDOEX, *Atmos. Chem. Phys.*, *3*, 563–579.

O'Dowd, C., M. H. Smith, I. E. Consterdine, and J. A. Lowe (1997), Marine aerosol, sea-salt, and the marine sulphur cycle: A short review, *Atmos. Environ.*, *31*(1), 73–80.

Patterson, C. C., and D. M. Settle (1976), The reduction of orders of magnitude errors in lead analysis of biological materials and natural waters by evaluating and controlling the extent and sources of industrial lead contamination introduced during sampling, collecting, handling and analysis, *Natl. Bur. Stand. Spec. Publ.*, *422*, 321–351.

Pszenny, A. A. P. (1992), Particle size distributions of methanesulfonate in the tropical Pacific marine boundary layer, *J. Atmos. Chem.*, *14*, 273–284.

Pszenny, A. A. P., W. C. Keene, D. J. Jacob, S. Fan, J. R. Maben, M. P. Zetwo, M. Springer-Young, and J. N. Galloway (1993), Evidence of inorganic chlorine gases other than hydrogen chloride in marine surface air, *Geophys. Res. Lett.*, *20*(8), 699–702.

Qian, G.-W., and Y. Ishizaka (1993), Electron microscope studies of methane sulfonic acid in individual aerosol particles, *J. Geophys. Res.*, *98*, 8459–8470.

Quinn, P. K., D. S. Covert, T. S. Bates, V. N. Kapustin, D. C. Ramsey-Bell, and L. M. McInnes (1993), Dimethylsulfide/cloud condensation nuclei/climate system: Relevant size-resolved measurements of the chemical and physical properties of atmospheric aerosol particles, *J. Geophys. Res.*, *98*, 10,411–10,427.

Rao, P., G. Momin, P. Safai, K. Ali, M. Naik, and A. Pillai (2001), Aerosol and trace gas studies at Pune during INDOEX IFP-99, *Curr. Sci.*, *80*, 105–109.

Reddy, M., and C. Venkataraman (2002a), Inventory of aerosol and sulphur dioxide emissions from India. Part II—Biomass combustion, *Atmos. Environ.*, *36*(4), 699–712.

Reddy, M., and C. Venkataraman (2002b), Inventory of aerosol and sulphur dioxide emissions from India: Part I—Fossil fuel combustion, *Atmos. Environ.*, *36*(4), 677–697.

Rhoads, K. P., P. Kelley, R. R. Dickerson, T. P. Carsey, M. Farmer, D. L. Savoie, and J. M. Porspero (1997), Composition of the troposphere over the Indian Ocean during the monsoonal transition, *J. Geophys. Res.*, *102*, 18,981–18,995.

Saltzman, E. S., D. L. Savoie, R. G. Zika, and J. M. Prospero (1983), Methane sulfonic acid in the marine atmosphere, *J. Geophys. Res.*, *88*, 10,897–10,902.

Saltzman, E. S., D. L. Savoie, J. M. Prospero, and R. G. Zika (1985), Atmospheric methanesulfonic acid and non-sea-salt sulfate at Fanning and American Samoa, *Geophys. Res. Lett.*, *12*(7), 437–440.

Sander, R., and P. J. Crutzen (1996), Model study indicating halogen activation and ozone destruction in polluted air masses transported to the sea, *J. Geophys. Res.*, *101*, 9121–9138.

Satsangi, G. S., A. Lakhani, P. Khare, S. P. Singh, K. M. Kumari, and S. S. Srivastava (2002), Measurements of major ion concentration in settled coarse particles and aerosols at a semiarid rural site in India, *Environ. Int.*, *28*(1–2), 1–7.

Savoie, D. L., and J. M. Prospero (1980), Water-soluble potassium, calcium, and magnesium in the aerosols over the tropical North Atlantic, *J. Geophys. Res.*, *85*, 385–392.

Savoie, D. L., and J. M. Prospero (1982), Particle size distribution of nitrate and sulfate in the marine atmosphere, *Geophys. Res. Lett.*, *9*(10), 1207–1210.

Savoie, D. L., and J. M. Prospero (1989), Comparison of oceanic and continental sources of non-sea-salt sulphate over the Pacific Ocean, *Nature*, *339*, 685–687.

Savoie, D. L., and J. M. Prospero (1994), Non-sea-salt sulfate and methanesulfonate at American Samoa, *J. Geophys. Res.*, *99*, 3587–3596.

Savoie, D. L., J. M. Prospero, and R. T. Nees (1987), Nitrate, non-sea-salt sulfate, and mineral aerosol over the northwestern Indian Ocean, *J. Geophys. Res.*, *92*, 933–942.

Savoie, D. L., R. Arimoto, W. C. Keene, J. M. Prospero, R. A. Duce, and J. N. Galloway (2002), Marine biogenic and anthropogenic contributions to non-sea-salt sulfate in the marine boundary layer over the North Atlantic, *J. Geophys. Res.*, *107*(D18), 4356, doi:10.1029/2001JD000970.

Siefert, R. L., A. M. Johansen, and M. R. Hoffmann (1999), Chemical characterization of ambient aerosol collected during the southwest and intermonsoon seasons over the Arabian Sea: Labile-Fe(II) and other trace metals, *J. Geophys. Res.*, *104*, 3511–3526.

Sievering, H., G. Ennis, E. Gorman, and C. Nagamoto (1990), Size distribution and statistical analysis of nitrate, excess sulfate, and chloride deficit in the marine boundary layer during GCE/CASE/WATOX, *Global Biogeochem. Cycles*, *4*(4), 395–405.

Sisterson, D. L. (1989), A method for evaluation of acidic sulfate and nitrate in precipitation, *Water Air Soil Pollut.*, *43*, 61–72.

Stickel, R. E., J. M. Nicovich, Z. Zhao, and P. H. Wine (1992), Kinetic and mechanistic study of the reaction of atomic chlorine with dimethyl sulfide, *J. Phys. Chem.*, *96*, 9875–9883.

Tindale, N. W., and P. P. Pease (1999), Aerosols over the Arabian Sea: Atmospheric transport pathways and concentrations of dust and sea salt, *Deep Sea Res., Part II*, *46*, 1577–1595.

Turnipseed, A. A., and A. R. Ravishankara (1993), The atmospheric oxidation of dimethyl sulfide: Elementary steps in a complex mechanism, in *Dimethylsulfide: Oceans, Atmosphere and Climate*, edited by G. R. A. G. Angeletti, pp. 185–196, Kluwer Acad., Norwell, Mass.

Venkataraman, C., P. Sinha, and S. Bammi (2001), Sulphate aerosol size distributions at Mumbai, India, during the INDOEX-FFP (1998), *Atmos. Environ.*, *35*(15), 2647–2655.

Venkataraman, C., C. Reddy, S. Josson, and M. Reddy (2002), Aerosol size and chemical characteristics at Mumbai, India, during the INDOEX-IFP (1999), *Atmos. Environ.*, *36*(12), 1979–1997.

Vogt, R., P. J. Crutzen, and R. Sander (1996), A mechanism for halogen release in the remote marine boundary layer, *Nature*, *383*, 327–330.

Yin, F., D. Grosjean, and J. H. Seinfeld (1986), Analysis of atmopheric photooxidation mechanisms for organosulfur compounds, *J. Geophys. Res.*, *91*, 14,417–14,438.

Yin, F., D. Grosjean, and J. H. Seinfeld (1990), Photooxidation of dimethyl sulfide and dimethyl disulfide. I: Mechanism development, *J. Atmos. Chem.*, *11*, 309–364.

M. R. Hoffmann, Environmental Science and Engineering, California Institute of Technology, Pasadena, CA 91125, USA.

A. M. Johansen, Department of Chemistry, Central Washington University, Ellensburg, WA 98826, USA. (johansea@cwu.edu)